PCCP

Accepted Manuscript

ROYAL SOCIETY OF CHEMISTRY

www.rsc.org/pccp

Journal Name

ARTICLE TYPE

Cite this: DOI: 10.1039/xxxxxxxxxx

High Resolution Triple Resonance Micro Magic Angle Spinning NMR Spectroscopy of Nanoliter Sample Volumes

J. Ole Brauckmann,[a,b] J.W.G. (Hans) Janssen,[a] and Arno P.M. Kentgens*[a]

Received Date
Accepted Date

DOI: 10.1039/xxxxxxxxxx

www.rsc.org/journalname

To be able to study mass-limited samples and small single crystals a triple resonance micro-magic angle spinning (μMAS) probehead for the application of high-resolution solid state NMR of nanoliter samples was developed. Due to its excellent rf performance this allows us to explore the limits of proton NMR resolution in strongly coupled solids. Using homonuclear decoupling we obtain unprecedented ^{1}H linewidhts for a single crystal of glycine ($\Delta\nu(CH_2)$ = 0.14 ppm) at high field (20 T) in a directly detected spectrum. The triple channel design allowed the recording of high-resolution μMAS ^{13}C-^{15}N correlations of [U-^{13}C-^{15}N] Arginine HCl and shows that the superior ^{1}H resolution opens the way for high-sensitivity inverse detection of heteronuclei even at moderate spinning speeds and rf-fields. Efficient decoupling leads to long coherence times which can be exploited in many correlation experiments.

1 Introduction

Solid-state NMR is often used to study isotopes occurring in low natural abundance. This requires expensive isotopic enrichment, or long experiment times where isotope labeling is not feasible. For sensitivity reasons it is best to study protons, in view of their high gyromagnetic ratio and their high natural abundance. The high gyromagnetic ratio of protons is exploited in liquid-state NMR experiments, where almost all heteronuclear experiments use proton detection generally referred to as inverse detection. In the solid state, however, protons form a strong dipolar coupling network that limits the achievable resolution. Currently there are three ways to obtain high-resolution proton spectra in the solid state: dilution of the protons by a high degree of deuteration, (fast) magic-angle spinning (MAS) and homonuclear decoupling. Partial deuteration of the sample leads to the highest proton resolution in the solid state, and has therefore attracted increasing attention for the study of large biomolecules.[1,2] Since the effective dipolar couplings are reduced by deuteration, the ^{1}H resolution obtained in this way is not comparable to the resolution obtained by fast MAS only or homonuclear decoupling of "fully protonated" systems. Furthermore the sensitivity in heteronuclear experiments is reduced and one has to resort to polarization transfer from ^{2}H, a quadrupolar nuclei, to carbon or nitrogen.[3]

MAS relies on the spatial dependence of the dipolar interaction. To be effective, the spinning speed should exceed the strength of the ^{1}H-^{1}H dipolar coupling. Recent hardware developments allow rotation frequencies beyond 100 kHz.[4] Despite spinning speeds up to 130 kHz[5], the highest resolution is still obtained using homonuclear decoupling by combined rotation and multiple pulse spectroscopy (CRAMPS).[6] In a recent publication it was estimated that spinning rates of about 250 kHz are needed to reach the linewidth of back-exchanged and deuterated samples.[7] CRAMPS techniques are designed for moderate spinning speeds, and the averaging is obtained mainly in spinspace. While PMLG/FSLG schemes[8,9] are based on average Hamiltonian theory,[10] the DUMBO sequences are numerically optimized decoupling sequences consisting of a phase modulation parametrized in a Fourier series. The first sequence (often referred to as DUMBO 1) was optimized using computer simulations.[11] The later so called experimental DUMBO versions (eDUMBO and PLUS-1) are

[a] Institute of Molecules and Materials, Radboud University, 6500 GL Nijmegen
[b] TI-COAST, Science Park 904, 1098 XH Amsterdam
* Corresponding author: Tel: +31 24 36 52078; E-mail: a.kentgens@nmr.ru.nl

† Electronic Supplementary Information (ESI) available: [Info]. See DOI: 10.1039/b000000x/

optimized on the spectrometer to take experimental factors as the rf-inhomogeneity and phase glitches into account.[12,13] Later our group introduced an on-spectrometer optimization strategy using evolutionary algorithms to find the best decoupling shape. Using a microcoil setup at 9.4 T and a decoupling field of 680 kHz, a resolution of 0.51 ppm for a methylene proton was obtained. Recent work has been devoted to the application of CRAMPS techniques at ultra-fast spinning rates.[14,15] Examples are the PLUS-1, TIMES and TIMES$_0$ sequences developed for fast and ultra-fast MAS.[16]

To benchmark the resolution for different decoupling techniques, often glycine is studied since it is a well-defined system with strong dipolar couplings. Despite the increased spinning speed, higher external magnetic fields and many different CRAMPS techniques, the resolution did not significantly increase in recent years and obtaining ^{1}H resolution remains an active field of research.[17–20]

Earlier experiments have shown that the use of microcoils is especially suitable for homonuclear decoupling.[21] Compared to conventional NMR, microNMR (coil diameter $<$ 1 mm) benefits from higher B_1 homogeneity over the sample and higher sensitivity since the signal to noise ratio is inversely proportional to the coil diameter.[22] The miniaturization of the coils allows one to reach exceptionally high rf-fields beneficial for the excitation of quadrupolar nuclei[23] and achieving smaller homogeneous linewidths for strongly coupled nuclei.[24] In addition, the miniaturization allows the study of mass-limited and selected samples. As was recently beautifully illustrated by Wong et al. in the study of metabolic profiles of individual cells.[25]

Inspired by the success of the earlier microcoil setup[21,24,26,27], we designed this novel triple resonance microMAS probe. In this paper we describe the specifications of the new micro triple tunable probe and present the first results of high-resolution solid-state NMR of nanoliter sample volumes in one- and two-dimensional experiments aimed at studying organic solids, polymers and pharmaceuticals. The triple-tuned setup was used in a ^{13}C -^{15}N correlation spectrum of uniformly labeled Arginine HCl. As we will describe, this leads to unprecedented resolution in proton and carbon spectra for strongly coupled spin-systems in the solid state.

The sensitivity of low-abundant nuclei can be enhanced by inverse detection.[28–30] The advent of ultra-fast magic angle spinning ($>$ 100 kHz) averages the dipolar interactions to an extent that permits the implementation of pulse sequences using the scalar couplings for polarization transfer in the solid state.[18,31] Recent work has shown that at fast spinning speeds the proton linewidth is sufficiently narrowed to obtain a sensitivity gain in inverse detection experiments in the solid-state. Following the theoretical derivation by Tycko et al., the sensitivity enhancement ξ is given by equation 1 and should lead to significant enhancements in the solid state.

$$\xi = C \cdot \left(\frac{\gamma_H}{\gamma_X}\right)^{\frac{3}{2}} \left(\frac{\Delta W_X}{\Delta W_H}\right)^{\frac{1}{2}} \quad (1)$$

Here C is a constant that depends on the quality factors of the coil for the different nuclei, and is influenced by constants such as the temperature, the coil geometry, filling factor etc. ΔW_X and ΔW_H are the natural linewidths of the X nuclei and the protons.[28] The actual enhancement reached is generally far below the theoretical maximum.

In this paper we show that substantial sensitivity gains can be obtained even at moderate spinning speeds, when homonuclear decoupling is used for line narrowing. We show that this combination results in correlation spectra with very high resolution and sensitivity.

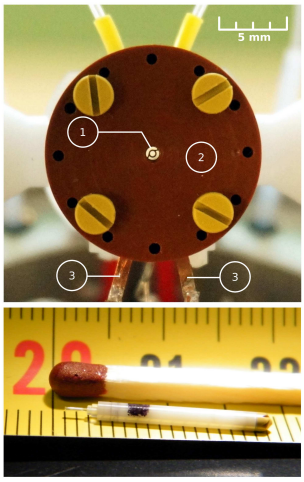

Fig. 1 Top: view onto the stator and the microcoil the numbers in the figure refer to 1) 375 μm copper microcoil (light shines through the coil), 2) the Vespel construction to hold the microcoil and 3) the contacts to the microcoil. Bottom: a 1.6 mm rotor with a filled microtip mounted onto the rotor is shown. The rotor is placed on a metric ruler with subdivisions in millimetres together with a match as well known size reference.

2 Experimental

2.1 a) Probe

The microMAS probehead used in this work is designed following the same principles described as "piggy-backed" in earlier work.[26,27]. A hand wound solenoid microcoil is integrated into a layered vespel construction mounted on a modified 1.6 mm Varian MAS pencil stator. The rf-coil is made from an isolated copper wire with a diameter of 100 μm (115 μm with coating). The wire is wound into 10 turns. The outer and inner diameter are 605 and 375 μm respectively. The triply-tunable rf circuit of the microcoil provides a ^{1}H channel tunable at 850 MHz with Q(^{1}H) = 130 , Q(^{13}C) = 75 at 213.7 MHz and Q(^{15}N) = 60 at 86.6 MHz

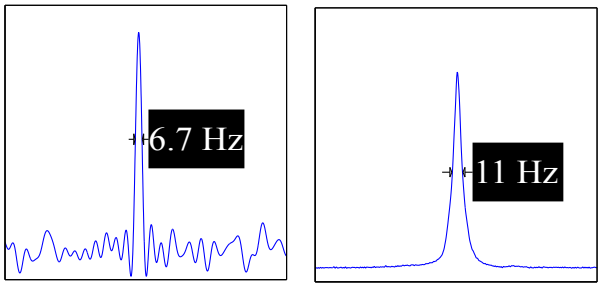

Fig. 2 Left: carbon spectrum of silicone rubber plug at 20 T using 5.2 kHz spinning and a decoupling field of 34 kHz. Right: proton spectrum of silicone rubber at 5.2 kHz (without decoupling).

resonance frequency. In figure 1 a view onto the stator and the dimensions of the rotor and the microtip are displayed. A picture of the probehead together with the circuitry used to connect the micro-coil is shown in figure S4. For the X channel we measured a tuning range of 60 MHz from 163.4 to 224.1 MHz. For the Y channel the range is narrower since more capacitors are used to reach the lower frequencies. The probe can be easily changed to other frequency ranges by changing the capacitors in the tuning circuitry.

For a proton-free background capillaries of fused silica are used as rotors. The outer and inner diameter are 320 μm and 250 μm respectively. Similar to the earlier design, the capillaries are mounted on a Kel-F holder that tightly fits into the 1.6 mm Varian rotor replacing the vespel end-cap. To limit the sample volume to the detection volume of the coil, a Kel-F spacer is inserted into the capillaries. This leaves sample heights of 800-1000 μm or corresponding sample volumes of 40-50 nanoliters. The top of the capillaries is closed with Teflon tape or UV glue. The back of the 1.6 mm pencil type stator is modified to allow loading of the rotor with the piggy-backed micro-rotor attached. The height of the rotor in the stator can be adjusted to align the sample at the center of the microcoil and to ensure stable spinning. Spinning speeds up to 20 kHz can be reached. The regular coil of the 1.6 mm stator is connected to a separate circuit tuned for X-nuclei observation e.g. for adjustment of the magic angle. In a system with dual receivers, running simultaneous experiments in the micro- and macro-rotor are feasible.

Compared to the earlier design, the sample lies in the center of the shim coils allowing improved shimming. Due to the small dimensions strong field variations of the shims are needed to affect the small detection volume. We optimized the shimming on a sample of silicon rubber in the center of the coil and achieved a full width at half height (FWHH) of 11 Hz for protons and of less than 6.7 Hz for carbons (2). Compared to the earlier design, the proton linewidth is half the value in Hertz at double the field (11 Hz here, compared to 20 Hz earlier).

Due to the small diameter very high rf-fields can be generated. Table 1 lists the rf-fields on all the three channels as a function of the input power.

2.2 b) Solid-State NMR experiments

All experiments were done on a Varian NMR System at an external field of 20 T (849.71 MHz proton frequency). For single pulse excitation spectra a 90^o pulse of 1.85 μs was used. For homonuclear decoupling either the DUMBO-1 coefficients[11] or a set of coefficients obtained by an EASY-GOING DUMBO on spectrometer optimization in the μMAS probe was used (see supplementary material).[21] For the inverse detection experiments a uniformly labeled glycine sample was used employing a recycle delay of 5 seconds. The cross-polarization periods were 500 μs. The spectral width in the indirect dimension was 62.5 kHz, $t_{1,max}$ = 6 ms and 4 scans were accumulated per increment. For DUMBO and SPINAL64[32] decoupling during evolution a ^{1}H rf field strength of 140 kHz was employed. For arginine HCl the acquisition parameters are given in the captions. If not stated otherwise, no apodization was used during processing.

The pulse sequences used are shown in 3. For high-resolution proton spectra we used the sequence shown in 3a using supercycled windowed DUMBO (wDUMBO) acquisition.[21] The high resolution ^{13}C-^{1}H HetCor correlation spectra were recorded with the sequence shown in 3b. The ^{1}H polarization is transferred to carbon for chemical shift evolution; the polarization is transferred back to protons for high-resolution detection using a wDUMBO acquisition with the on-spectrometer optimized coefficients. The timings and the acquisition parameters are given in the caption of the spectra. A ^{13}C-^{15}N correlation was obtained with the sequence shown in 3c. Carbon polarization obtained by cross-polarization evolves before the transfer to nitrogen. The polarization is mixed under DARR irradiation[33] before acquisition. During evolution and acquisition protons are decoupled using SPINAL64 decoupling[32].

2.3 Samples

To handle the small dimension a set of filling tools was built to ease filling of the capillary. To center the sample to the detection volume of the coil the sample was packed in between of thin layers of quartz powder. The capillary was sealed either with Teflon tape or with a thin layer of UV-glue. Since the end of the capillary is outside of the microcoil, the influence on the spectra is minor, especially in CP experiments since the matching condition is optimized for the center of the coil.

U-[^{13}C,^{15}N] glycine and U-[^{13}C,^{15}N] L-Arginine HCl were purchased from Sigma Aldrich and used without further purification.

Table 1 RF fields as function of the power used.

^1H Power(W)	$\nu_{rf}(^1\mathrm{H})$ [kHz]	X Power[W]	$\nu_{rf}(^{13}\mathrm{C})$ [kHz]	Y Power[W]	$\nu_{rf}(^{15}\mathrm{N})$ [kHz]
1	146	2.4	45	7	46
3.3	277	18.9	140	31	141
10.2	506	85.2	300	100	211

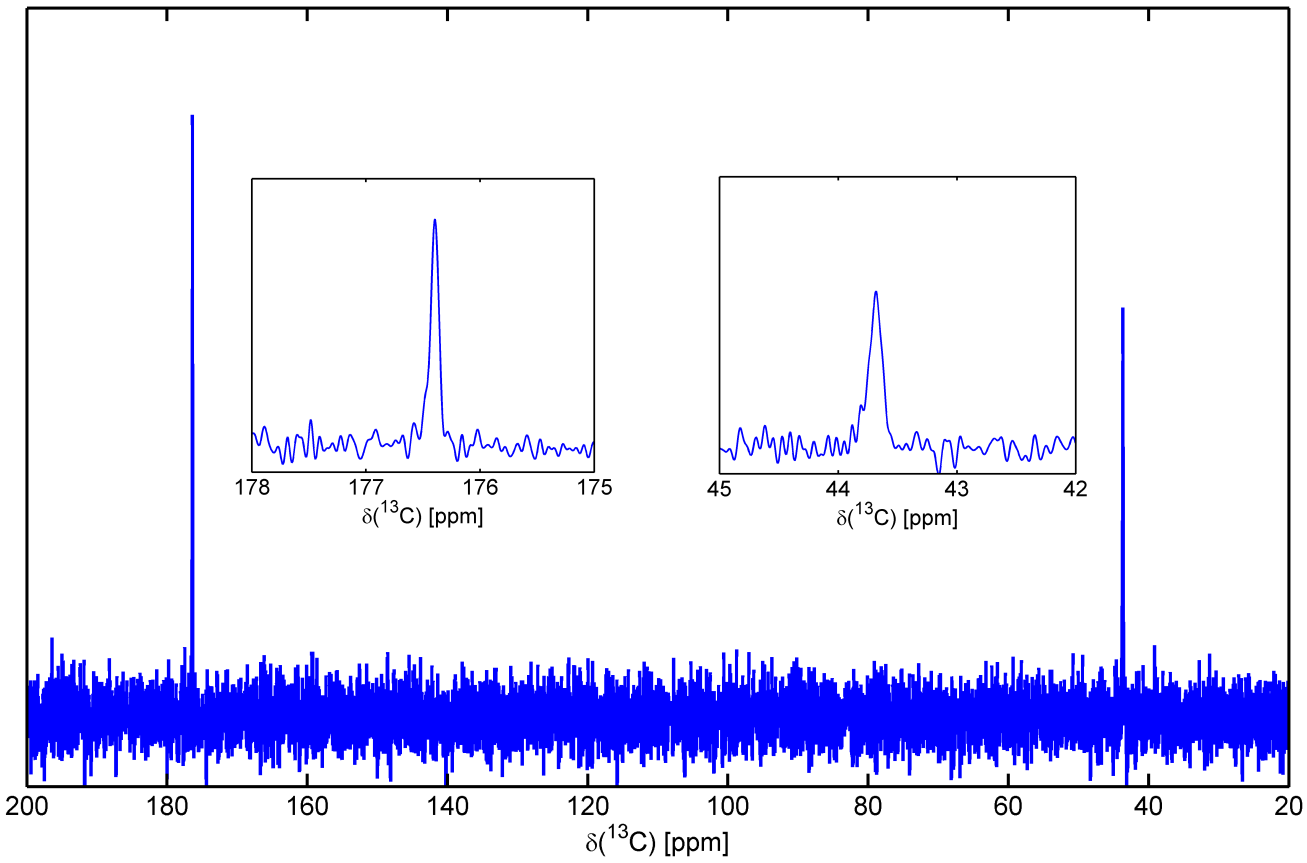

Fig. 4 ^{13}C CP MAS spectrum of a single crystal of 40 nL natural abundant glycine. The spectral regions shown in the insets are the carbonyl resonance (left) and the methylene group obtained from a nutation spectrum acquired with 128 scans per increment and Δt_1 = 7.5 μs ($t_{1,max}$=450 μs). During acquisition of 75 ms, 100 kHz SPINAL64 decoupling was used.

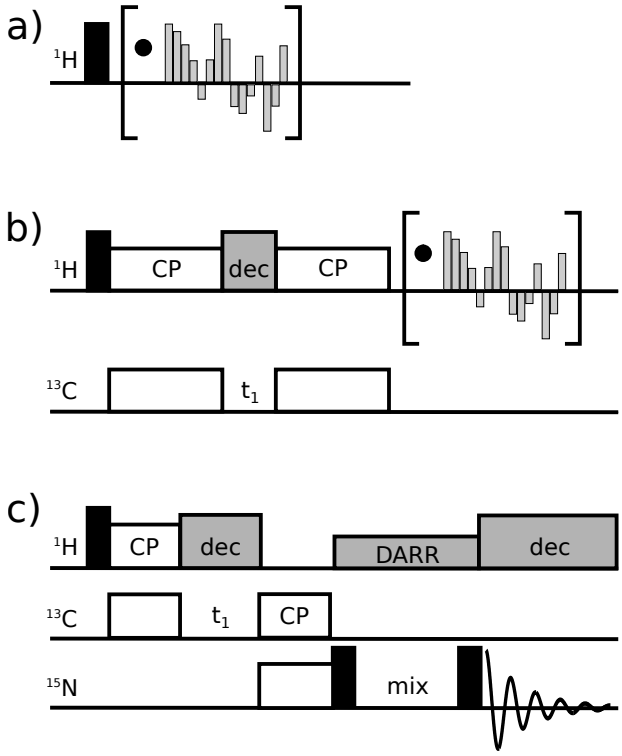

Fig. 3 Pulse sequences used a) wDUMBO acquisition b) inverse detection HetCor c) ^{13}C-^{15}N correlation using DARR mixing. A solid block indicates a 90 degree pulse, grey blocks are decoupling periods.

3 Results

3.1 Resolution

Vasa et al. have shown that the μMAS-approach has benefits for highly abundant nuclei. Especially homonuclear decoupling sequences as FSLG and DUMBO perform well.[27] Later it was shown that highly resolved proton DUMBO spectra can be obtained even at extreme rf fields of 680 kHz.[21] When the available proton fields are used for decoupling, exceptional long coherence lifetimes can be achieved.[24] This illustrates the added value of microcoils in the study of strongly coupled system e.g. in materials science. Since high rf fields are readily available, heteronuclear correlations with high power decoupling can be acquired. Vasa et al. have demonstrated, that if sufficient resolution for the involved nuclei can be obtained, heteronuclear correlations in natural abundance are in principle feasible in a reasonable amount of time.[27] To check the achievable resolution in the new μMAS probe, we start our investigation with the study of glycine. In 4 the ^{13}C CP MAS spectrum of a single crystal of natural abundant glycine is shown of approximately 40 nL volume. The acquisition parameters are given in the caption of the figure. The linewidth obtained for the carbonyl resonance is 16 Hz compared to 25.5 Hz for the methylene-carbon. Vasa et al. obtained a resolution of 15 Hz at 400 kHz rf for the methylene carbon at approximately half the magnetic field (9.4 T).

In 5 the homonuclear decoupled ^{1}H spectrum of natural abundant glycine powder using wDUMBO acquisition is shown. Using the optimized DUMBO coefficients, the resolution was slightly better compared to the DUMBO-1 coefficients.[11] The resolution obtained for the powder is well below 0.5 ppm for all the resonances (0.38-0.31 ppm), with the CH_2 protons resolved down to the baseline.

When the wDUMBO sequence using the DUMBO-1 coefficients is applied to a single crystal, the resolution increases drastically (6). For the methylene protons, the resolution improved from 0.31 to 0.14 ppm. The line narrowing is ascribed to the reduced anisotropic bulk magnetic susceptibility (ABMS) in a single crystal. The resolution obtained for the powder and the single crystal in ppm is much higher compared to the earlier μMAS setup. For the single-crystal we observe that the resolution in Hz at 20 T using much lower rf-fields is approximately twice as good as the resolution obtained at 9.4 T. The observed line-narrowing is in agreement with the observations on carbon measurements of a single crystal.[24]

3.2 Inverse Detection

Employing inverse detection the sensitivity of low abundant nuclei can be increased. When polarization transfer is efficient, detection of the signal at a higher gyromagnetic ratio increases the sensitivity. In the pioneering work of Tycko et al.[28] it was shown

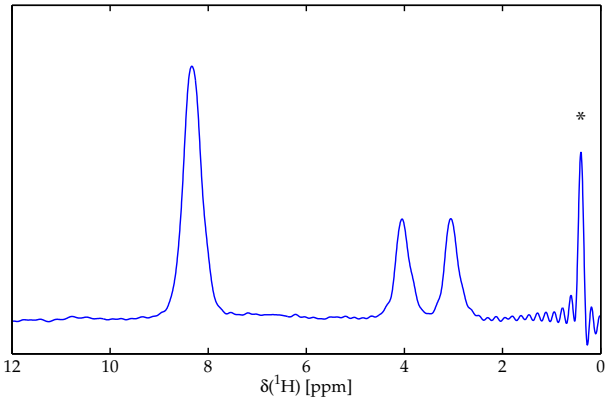

Fig. 5 ^{1}H spectrum of 50 nL natural abundant glycine powder using wDUMBO acquisition. Acquired using 4 scans at 12.5 kHz spinning, at 20 T external field and 140 kHz rf frequency. The rescaled ^{1}H linewidths are from left to right $\Delta\nu(NH_3^+)$ 330 Hz, $\Delta\nu(CH_2)$ 260 Hz and $\Delta\nu(CH_2)$ 266 Hz. The line on the right is an artefact at the carrier frequency.

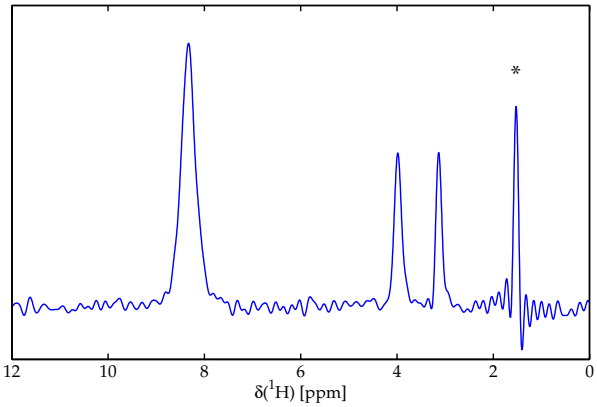

Fig. 6 ^{1}H wDUMBO spectrum of a 40 nL single crystal vr=12 kHz, DUMBO-1 coefficients. The spectrum was acquired using 4 scans at 12 kHz spinning, 20 T external field and a B_1 field of 140 kHz rf nutation frequency. The rescaled ^{1}H linewidths are from left to right $\Delta\nu(NH_3^+)$ 315 Hz, $\Delta\nu(CH_2)$ 165 Hz and $\Delta\nu(CH_2)$ 121 Hz. The line on the right is an artefact at the carrier frequency. No apodization was used during processing.

that the sensitivity enhancement depends on the linewidth of the nuclei. Since the narrowest lines are obtained with homonuclear decoupling, the use of homonuclear decoupling in combination with inverse detection should result in the highest sensitivity. So far not many examples reporting high sensitivity of this combination are found in literature,[30,34] probably due to the fact that most homonuclear techniques require relative high power resulting in heating of the sample due to the electrical field, with detrimental consequences for biological samples. However for the emerging field of NMR crystallography, pharmaceutical compounds, small organic molecules and material science this is a promising combination and no sample heating is expected.

In 7, a heteronuclear correlation of glycine is shown using inverse detection and wDUMBO acquisition. The proton dimension shows similar resolution than the direct DUMBO decoupled proton spectra of fully labeled samples (not shown). The resolution for a uniformly labeled sample is about 0.5 ppm in both dimensions. Considering the high carbon resolution in the indirect dimension is somewhat truncated ($t_{1,max}$ = 3.6 ms). The estimated resolution from an exponential fit of the full t_1 decay recorded in a separate experiment (Figure S1) indicates a T_2 of 5.07 $\pm$ 0.21 ms corresponding to a full width at half height of approximately 62.8 Hz or 0.3 ppm in the indirect dimension at the given field. The signal to noise for the carbon trace along the amine proton resonance in the correlation is about 200 in both dimensions. By comparison of the inverse detection HetCor spectrum to a carbon detected one acquired with similar acquisition parameters and the DUMBO decoupling in the indirect dimension, we estimate the sensitivity enhancement ξ defined in equation 1 to be around 5.1 fold (see suppl.).

3.3 Heteronuclear study of U-^{13}C,^{15}N L-Arginine HCl

One of the added values of the current probe design is the presence of a third channel in the micro setup. We measured ^{13}C and ^{15}N spectra of fully labeled L-Arginine HCl. In 8 the carbon spectrum is shown. The resonances agree with the assignment presented earlier in literature.[35,36] Since two molecules of arginine are present in the unit cell, two sets of resonances are observed except for the carbonyl and the C_ξ resonances which overlap. From right to left the resonances were assigned by Li et al to the C_γ, C_β resonances around 25 ppm. Followed by the C_δ resonances around 42 ppm and the C_α around 55 ppm. The C_ξ and the carbonyl species resonate at higher ppm values (156 and 176 ppm).[36] In 9 a ^{15}N CP MAS spectrum of Arginine HCl is shown. Also here a doubling of most resonances due to the two molecules in the unit cell is clearly visible. From right to left the resonances are assigned to the N_α the $N_{\eta 1}$ and $N_{\eta 2}$ and N_ξ atoms shown in the inset. The resonances agree with the resonances reported by the group of Hong.[36]

In 10 the ^{13}C-^{15}N correlation using double CP and 0.8 ms DARR mixing of the ^{15}N polarization is shown. Clear correlations of the expected resonances are seen. The N_ξ and N_η nitrogens show correlations with the C_ξ carbon, while the N_α shows only correlations with the α-carbons (compare insets).

4 Discussion

4.1 Carbon Resolution

The linewidth obtained for the carbon and proton spectra of the single crystal of glycine is narrower compared to the powdered sample. The linewidth in the carbon spectrum of the single crys-

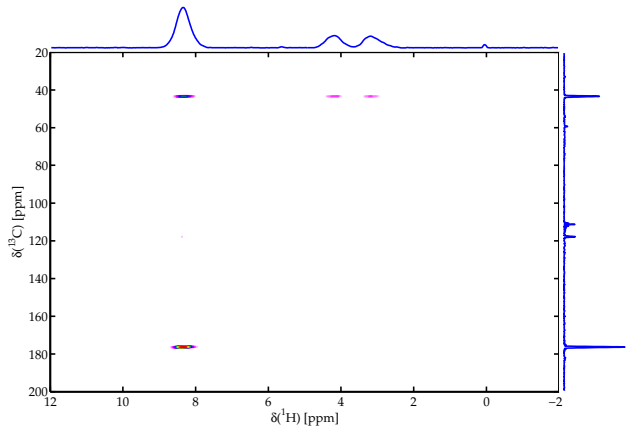

Fig. 7 Inverse detection ^{1}H-^{13}C HetCor of 50 nL [U-^{13}C,^{15}N] glycine using wDUMBO with EGD coefficients during acquisition. For both CP blocks (to carbon and back to protons) a contact time of 500 μs was used. 301 increments with 4 averages were collected following the States procedure in a total time of 3 h 22 min. The spectral width was 40.322 kHz and 50 kHz in the indirect dimension. For processing 20 Hz exponential line-broadening was applied in the direct dimension.

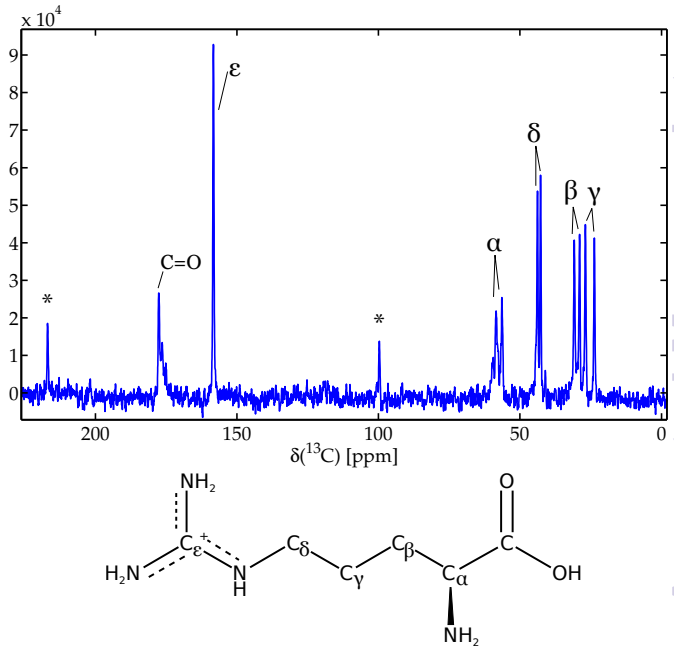

Fig. 8 ^{13}C CP MAS spectrum of 50 nL U-^{13}C-^{15}N L-Arginine HCl. 64 scans were acquired using a spectral width of 62.5 kHz and recycle delay of 100 sec. The contact time was 1.5 ms, the spinning speed 12.5 kHz. 140 kHz ν_{rf}^{H} was used for SPINAL64 decoupling. Astericses indicate spinning sidebands. The FID was apodized with 25 Hz exponential line-broadening. Above the spectrum, the structure of Arginine and the carbon assignment is shown.

tal of glycine for the CH_2 group is is 26 Hz at 20 T compared to 15 Hz earlier at about half the field (9.4 T),[24] *i.e.* in ppm the resolution is comparable.

In the solid state three different mechanisms contribute to the linewidth. The linewidth can consist of the residual dipolar couplings not averaged by MAS or decoupling, the anisotropic bulk magnetic susceptibility (ABMS) due to the packing of the differently shaped crystallites in the sample, and the chemical shift dispersion due to disorder in the sample. The ABMS is less in a single crystal and therefore the resolution in micro-crystalline systems and single crystals increases.[37] The ABMS broadening scales with the external field, whereas the residual dipolar couplings are approximately field independent. The fact that the linewidth in Hertz of the single crystal of glycine scales approximately linearly with the external magnetic field, indicates that the linewidth is not dominated by residual dipolar couplings, but is probably limited by susceptibility effects. Since we measure a good quality single crystal, the contribution from chemical dispersion is expected to be minor.

When the linewidth is dominated by susceptibility effects, the intrinsic resolution is probably much higher, as earlier experiments using decoupling fields up to 400 kHz already indicated.[24] Here, much lower decoupling fields of about 140 kHz were used. Increasing the decoupling fields might increase the resolution in Hertz further towards the extreme long coherence times indicated by the echo experiments in the earlier μMAS setup[24] and later using fast MAS and low-power decoupling.[38,39] Experiments in this direction will indicate what limits the resolution in the solid state. Long coherence times in the solid-state allow for more efficient polarization transfer in sequences using scalar-couplings.[38]

4.2 Proton Resolution

For the proton resolution of glycine under homonuclear decoupling we observe a similar linewidth reduction for the single crystal. For the powder a rescaled linewidth of about 260 Hz (0.31 ppm) is observed compared to 121 Hz (0.14 ppm) for the single crystal. To determine the chemical shift scaling factor we performed a 2D experiment correlating the ^{1}H MAS spectrum and the DUMBO-decoupled proton spectrum (compare Grimminck et al[21]). The scaling factor of 0.49 agrees with the convention used by Lu et al. to reference the NH_3^+ resonance to 8.33 ppm and the middle of the CH_2 resonances to 3.55 ppm.[15]

In recent years, a lot of research has been devoted to the development of ever faster spinning probes to increase the proton resolution. Fast spinning averages the dipolar couplings, but to date the best resolution is still obtained using CRAMPS techniques. At higher external field using DUMBO decoupling the resolution should increase, since the increased Zeeman interaction should more efficiently truncate the dipolar couplings among protons. However this was not experimentally observed

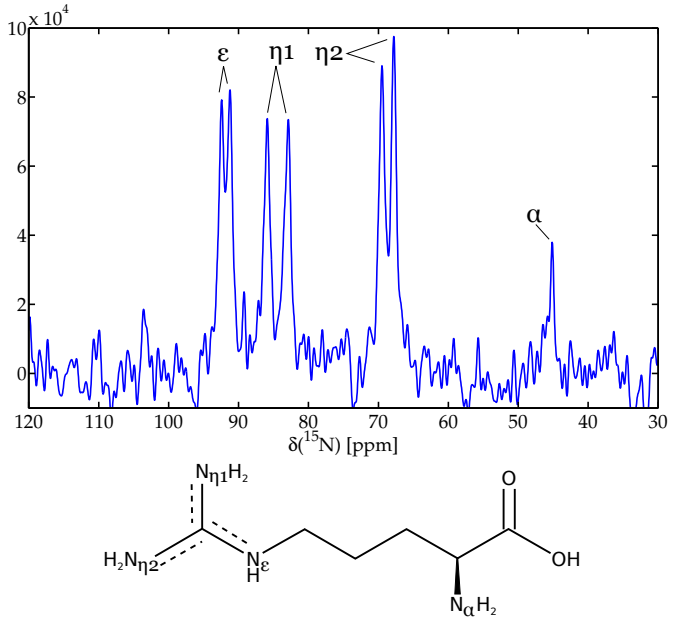

Fig. 9 ^{15}N CP MAS spectrum of 50 nL U ^{13}C-^{15}N L-Argine HCl. Here a spectral width of 25 kHz and a contact time of 2 ms was used at 12.5 kHz spinning. Again 64 scans with a recycle delay of 100 sec were used. The proton decoupling field ν_{rf}^{H} was 140 kHz for SPINAL64 decoupling. Above the spectrum, the structure of Arginine and the nitrogen assignment is shown. 25 Hz exponential line-broadening was applied.

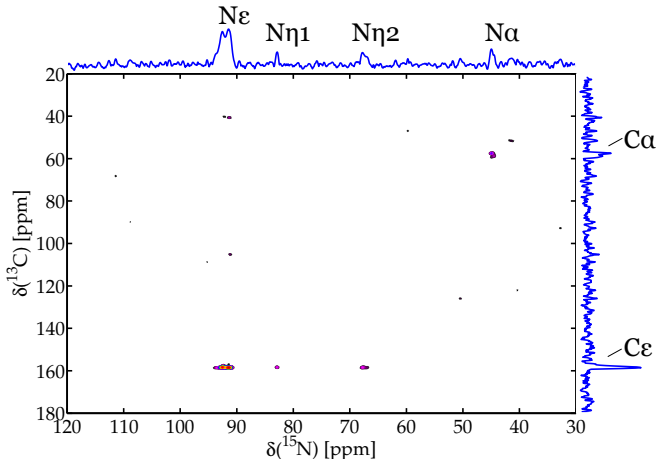

Fig. 10 ^{13}C-^{15}N correlation of 50 nL U ^{13}C-^{15}N L-Arginine HCl. Here 96 increments following the States procedure with 16 scans per increment and a recycle delay of 60 seconds were acquired. The contact time to carbons was 1 ms and to nitrogen 2.5 ms. The DARR mixing period was set to 0.8 ms. The spinning frequency was 12.5 kHz during acquisition, SPINAL64 decoupling of 140 kHz ν_{rf}^{H} was applied. For apodization 50 Hz exponential line-broadening was applied in both dimensions.

in homonuclear decoupling experiments at higher external magnetic fields.[40] Whereas, in MAS only proton spectra this is clearly observed.[7,41]

When the resolution obtained here is compared to the literature, care should be taken, since often the resolution in the indirect dimension, or polarization selected by a 810^o pulse is reported[15]. Here we report the resolution of direct acquisition experiments using the wDUMBO sequence.

Earlier, Lesage et. al reported the resolution obtained for the CH resonance in L-alanine acquired in the indirect dimension at different fields (400, 600 and 750 MHz).[40] The best resolution obtained was obtained at 600 MHz (160 Hz, 0.26 ppm compared to 260 Hz, 0.34 ppm at 750MHz). Using constant time acquisition the resolution improves to 130 Hz (0.17 ppm). Later Salager et al. reported a resolution of 230 Hz (0.47 ppm) at 500 MHz and 65 kHz spinning.[42] Fast spinning improves the sensitivity of DUMBO-acquisition if resonance conditions of the DUMBO-cycle and the rotor-period are avoided.[13,40,42] DUMBO experiments at different spinning speeds indicate that the resolution does not increase at high spinning speeds, but the intensity changes.[42] At fast MAS (>60 kHz) and high field, Salager obtained a resolution of 269 Hz (0.34 ppm) and 239 Hz (0.24 ppm) at 1 GHz using windowed acquisition and the PLUS-1 sequence.[13] However in these measurements, only the center part of a 1.3 mm rotor was filled making the comparison to other experiments difficult.

For the powder at 850 MHz we obtain a very high resolution using windowed acquisition at relative low spinning speeds and mild rf-conditions for state-of-the-art rf-probes. We note that the 810^o pulse, does not significantly improve the resolution, proving good B_1 homogeneity over the sample volume. The homogeneity is confirmed in a nutation experiment with A_{810}/A_{90} = 98.1 %. A detailed description of the B_1 homogeneity is given in the supplementary material.

For the single crystal the DUMBO-1 coefficients[11] at 12 kHz spinning and 140 kHz rf were used. These results clearly show that for proton resolution the study of single-crystal samples might increase the resolution significantly. The proton resolution obtained here exceeds the resolution obtained at ultra-fast MAS and high-field.

Good homonuclear decoupling results have been obtained before using a microcoil setup and optimization of the DUMBO-coefficients at very high rf-fields up to 680 kHz.[21] Increased rf-fields and on-spectrometer optimization might increase the resolution further. In principle higher rf-fields will allow to more efficiently decouple even stronger dipolar interactions. However at higher fields rf-heating might play a roll. But it was recently demonstrated that rf-heating may be alleviated by cooling a microcoil with an internal liquid flow.[43] This also allows susceptibility matching of the coil allowing even higher resolution. Investigations along these lines are underway.

The resolution obtained for the powder and the single crystal al-

lows us to use the proton chemical shift for structural studies in the solid-state, *e.g.* in high resolution correlation experiments. For a long time in solid-state NMR, mostly X nuclei were used for structure elucidation, because strong homonuclear couplings of protons limit the attainable resolution, and many resonances overlap in the relatively small chemical shift range of protons. With the advent of homonuclear decoupling and especially ever faster spinning probes, the proton chemical shift becomes more and more accessible for structure elucidation. In the field of NMR crystallography proton chemical shifts are exploited.[44] Recent examples show that the proton chemical shifts are more sensitive to structural changes than carbon chemical shifts and allow better discrimination between structural models as carbon chemical shifts.[45] Also in biosolid-state NMR recent examples of ultra-fast MAS make use of the increased proton resolution and the high sensitivity by proton detection.[18,19] However still proton dilution is used for sufficient resolution. In biosolid-state NMR, high power homonuclear decoupling schemes are often not viable due to sample heating. Therefore still commonly expensive proton dilution by partial deuteration of the sample is applied. If rf-heating can be controlled, using homonuclear decoupling in correlation experiments, the sensitivity can be significantly increased using fully protonated samples especially when combined with inverse detection. The development of new techniques combining fast magic angle spinning with homonuclear decoupling has brought advances such as broader spectral widths in the indirect dimensions for rotor synchronized experiments, but the progress in resolution since the reports of the eDUMBO versions lack the expected linear factor by the B_0-field.

4.3 Arginine HCl

The CP-MAS carbon and nitrogen spectra reflect the benefit of the new probe design. High resolution carbon and nitrogen spectra of minute quantities can be obtained with a resolution comparable to state-of-the-art commercial probes. Since two molecules of Arginine are in the unit cell,[46] the amount of molecules detected is about 150 nanomols or an equivalent of about 26 μg. The carbon nitrogen correlation demonstrates that the new μMAS probe enables us to do high resolution triple resonance spectroscopy of mass-limited samples (up to 50 nL volume), even allowing ^{13}C-^{15}N correlation experiments labeled compounds. The resolution is comparable to commercial setups for labeled samples.

4.4 Inverse Detection

In solid-state inverse detection experiments, the sensitivity gain strongly depends on the proton linewidth. Therefore, most examples use fast magic angle spinning[28,41,47,48] and more recently ultrafast MAS.[18,19,30,31,49] At ultrafast spinning HSQC type schemes using transfer by scalar couplings become available due to longer proton coherence times.[30,31,49] The enhancement reached is mostly far below the theoretical maximum. Following the theoretical derivation by Tycko et al., a maximum sensitivity enhancements, of about eight could be reached in 2D experiments for carbon as heteronucleus. In principle substantial sensitivity gains should also be achieved if CRAMPS techniques are applied to narrow the proton linewidth.

To our knowledge there have so far been no reports on the combination of low spinning speeds and homonuclear decoupling using conventional probes. The only other example used also a microcoil.[27] A recent report combined homonuclear decoupling and fast spinning,[30] demonstrating the feasibility of this combination. However in this study protons and nitrogens were correlated. Earlier heteronuclear combinations were reported but without reporting the sensitivity enhancement.[34]

So far, most studies focus on the heteronuclear correlation of nitrogen and protons since the higher ratio of the involved gyromagnetic ratios allows for a higher sensitivity gain $(\gamma_{H^1}/\gamma_{N^{15}})^{3/2} \sim 31$.[28,30,47,50] Examples using proton carbon correlations had difficulties reaching a sensitivity gain. At 40 kHz spinning speeds for a proton carbon correlations a sensitivity gain of 3.6 were observed[41] compared to 2-3 in first reports.[29]

By comparing a carbon detected HetCor and proton detected HetCor experiment with comparable acquisition parameters, we estimate the sensitivity gain in our experiments to be 5.1 (suppl). The DUMBO coefficients used for the comparison are the DUMBO-1 coefficients. The sensitivity gain obtained in the current study is substantially higher at much lower spinning speed and is in the range of the enhancements reached with ultrafast MAS schemes. These experiments allow one to study mass-limited samples and small molecules with high resolution and sensitivity. The observation made by Lesage and Salager, that the proton signal intensity under DUMBO-decoupling increases at increased spinning speeds,[40,42] might increase the sensitivity further towards the theoretical maximum enhancement of eight given by the ratio of the gyromagnetic constants.

However the signal to noise ratio of the proton detected HetCor spectrum of 50 nL uniformely labeled glycine shown in 7 is already about 200 in the experiment time of 3 hours 22 min. This means that heteronuclear correlation experiments for small molecules are feasible in an over night experiment in natural abundance, even for such small volumes of 50 nL. In natural abundance the signal loss will be not a factor 100, since the proton linewidth under homonclear is less and for carbons the linesplittings are reduced, due to the absence of homo- and heteronuclear scalar couplings. Therefore the present setup opens the road for novel applications as NMR crystallography since only minute quantities are required and precise chemical shifts are required for the discrimination between different structures. The high resolution is also useful for the study of polymorphism since only small quantities are needed, the probe allows the study of small

individual crystals, or the study of selected regions of a macroscopic sample for instance in materials science.

5 Conclusions

We present the first triple resonance micro magic angle spinning setup, which offers a significant improvement in resolution thus opening novel applications allowing novel experiments that need very long coherence life times. The probe allows the study of mass-limited and selected samples with highest resolution and high sensitivity. Being a micro-setup, sample volumes of only 50 nL are needed. The high rf-fields reached bear great promise for heteronuclear and homonuclear decoupling and the study of quadrupolar nuclei due to higher excitation efficiencies at higher rf-fields. The proton resolution of 0.14 ppm for a natural abundant single crystal of glycine at high field is unprecedented. We have shown that the combination of line-narrowing by homonuclear decoupling in inverse detection experiments allows substantial enhancements ($\xi \sim 5$)for ^{1}H-^{13}C correlations even at moderate spinning speeds. The triple channel setup and the good resolution in combination with sensitive proton detection experiments allows the use of proton chemical shifts in structural studies (NMR crystallography) of pharmaceutical compounds and small organic molecules. Furthermore the the signal to noise ratio in the inverse detection experiments allows the study of heteronuclear correlation of small molecules even in natural abundance.

6 Acknowledgement

The authors thank Jan van Os for his technical support. The Netherlands Organization for Scientific Research (NWO) is acknowledged for their financial support of the solid-state NMR facility for advanced material science. Edwin Sweers is acknowledged for the micro-fabrication of the Kel-F holder used to mount the micro-rotor on the 1.6 mm rotor. This research received funding from the Netherlands Organization for Scientific Research (NWO) in the framework of the Technology Area COAST.

References

1 A. E. McDermott, F. J. Creuzet, A. C. Kolbert and R. G. Griffin, *J. Magn. Res.*, 1992, **98**, 408–413.

2 Ü. Akbey, S. Lange, W. T. Franks, R. Linser, K. Rehbein, A. Diehl, B.-J. v. Rossum, B. Reif and H. Oschkinat, *J. Biomol. NMR*, 2009, **46**, 67–73.

3 D. Wei, Ü. Akbey, B. Paaske, H. Oschkinat, B. Reif, M. Bjerring and N. C. Nielsen, *J. Phys. Chem. Lett.*, 2011, **2**, 1289–1294.

4 Y. Q. Ye, M. Malon, C. Martineau, F. Taulelle and Y. Nishiyama, *J. Magn. Res.*, 2014, **239**, 75–80.

5 A. Samoson, *EUROMAR 2015*, 2015, P 036.

6 L. Wang and D. H. Zhou, *J. Magn. Res.*, 2013, **234**, 141–146.

7 A. Böckmann, M. Ernst and B. H. Meier, *J. Magn. Reson.*, 2015, **253**, 71–79.

8 M. Lee and W. I. Goldburg, *Phys. Rev.*, 1965, **140**, A1261.

9 E. Vinogradov, P. Madhu and S. Vega, *Chem. Phys. Lett.*, 1999, **314**, 443–450.

10 U. Haeberlen and J. S. Waugh, *Phys. Rev.*, 1968, **175**, 453–467.

11 D. Sakellariou, A. Lesage, P. Hodgkinson and L. Emsley, *Chem. Phys. Lett.*, 2000, **319**, 253–260.

12 B. Elena, G. de Paëpe and L. Emsley, *Chem. Phys. Lett.*, 2004, **398**, 532–538.

13 E. Salager, J.-N. Dumez, R. S. Stein, S. Steuernagel, A. Lesage, B. Elena-Herrmann and L. Emsley, *Chem. Phys. Lett.*, 2010, **498**, 214–220.

14 M. Leskes, S. Steuernagel, D. Schneider, P. Madhu and S. Vega, *Chem. Phys. Lett.*, 2008, **466**, 95–99.

15 X. Lu, O. Lafon, J. Trébosc, A. S. L. Thankamony, Y. Nishiyama, Z. Gan, P. K. Madhu and J.-P. Amoureux, *J. Magn. Res.*, 2012, **223**, 219–227.

16 Z. Gan, P. K. Madhu, J.-P. Amoureux, J. Trébosc and O. Lafon, *Chem. Phys. Lett.*, 2011, **503**, 167–170.

17 M. E. Halse and L. Emsley, *J. Phys. Chem. A*, 2013, **117**, 5280–5290.

18 E. Barbet-Massin, A. J. Pell, J. S. Retel, L. B. Andreas, K. Jaudzems, W. T. Franks, A. J. Nieuwkoop, M. Hiller, V. Higman, P. Guerry, A. Bertarello, M. J. Knight, M. Felletti, T. Le Marchand, S. Kotelovica, I. Akopjana, K. Tars, M. Stoppini, V. Bellotti, M. Bolognesi, S. Ricagno, J. J. Chou, R. G. Griffin, H. Oschkinat, A. Lesage, L. Emsley, T. Herrmann and G. Pintacuda, *J. Am. Chem. Soc.*, 2014, **136**, 12489–12497.

19 V. Agarwal, S. Penzel, K. Szekely, R. Cadalbert, E. Testori, A. Oss, J. Past, A. Samoson, M. Ernst, A. Böckmann and B. H. Meier, *Angew. Chem. Int. Ed.*, 2014, **53**, 12253–12256.

20 D. H. Brouwer and M. Horvath, *Solid State Nucl. Magn. Reson.*, 2015.

21 D. L. Grimminck, S. K. Vasa, W. L. Meerts, A. P. Kentgens and A. Brinkmann, *Chem. Phys. Lett.*, 2011, **509**, 186–191.

22 A. P. M. Kentgens, J. Bart, P. J. M. v. Bentum, A. Brinkmann, E. R. H. v. Eck, J. G. E. Gardeniers, J. W. G. Janssen, P. Knijn, S. Vasa and M. H. W. Verkuijlen, *J. Chem. Phys.*, 2008, **128**, 052202.

23 M. Inukai and K. Takeda, *Concepts Magn. Reson.*, 2008, **33B**, 115–123.

24 S. K. Vasa, H. Janssen, E. R. H. V. Eck and A. P. M. Kentgens, *Phys. Chem. Chem. Phys.*, 2010, **13**, 104–106.

25 A. Wong, C. Boutin and P. M. Aguiar, *Front. Chem.*, 2014, **2**, 38.

26 H. Janssen, A. Brinkmann, E. R. H. van Eck, P. J. M. van Bentum and A. P. M. Kentgens, *J. Am. Chem. Soc.*, 2006, **128**, 8722–8723.

27 A. Brinkmann, S. K. Vasa, H. Janssen and A. P. M. Kentgens,

Chem. Phys. Lett., 2010, **485**, 275–280.
28 Y. Ishii and R. Tycko, *J. Magn. Res.*, 2000, **142**, 199–204.
29 Y. Ishii, J. P. Yesinowski and R. Tycko, *J. Am. Chem. Soc.*, 2001, **123**, 2921–2922.
30 S. M. Althaus, K. Mao, J. A. Stringer, T. Kobayashi and M. Pruski, *Solid State Nucl. Magn. Reson.*, 2014, **57–58**, 17–21.
31 G. P. Holland, B. R. Cherry, J. E. Jenkins and J. L. Yarger, *J. Magn. Reson.*, 2010, **202**, 64.
32 B. M. Fung, A. K. Khitrin and K. Ermolaev, *J. Magn. Reson.*, 2000, **142**, 97–101.
33 K. Takegoshi, S. Nakamura and T. Terao, *Chem. Phys. Lett.*, 2001, **344**, 631–637.
34 T. Kobayashi, K. Mao, P. Paluch, A. Nowak-Król, J. Sniechowska, Y. Nishiyama, D. T. Gryko, M. J. Potrzebowski and M. Pruski, *Angew. Chem. Int. Ed.*, 2013, **52**, 14108–14111.
35 A. T. Petkova, J. G. Hu, M. Bizounok, M. Simpson, R. G. Griffin and J. Herzfeld, *Biochemistry*, 1999, **38**, 1562–1572.
36 S. Li, Y. Su, W. Luo and M. Hong, *J. Phys. Chem. B*, 2010, **114**, 4063–4069.
37 D. Vanderhart, W. L. Earl and A. Garroway, *J. Magn. Reson.*, 1981, **44**, 361–401.
38 J. R. Lewandowski, J.-N. Dumez, Ü. Akbey, S. Lange, L. Emsley and H. Oschkinat, *J. Phys. Chem. Lett.*, 2011, **2**, 2205–2211.
39 V. Agarwal, T. Tuherm, A. Reinhold, J. Past, A. Samoson, M. Ernst and B. H. Meier, *J. Chem. Phys. Lett.*, 2013, **583**, 1–7.
40 A. Lesage, D. Sakellariou, S. Hediger, B. Eléna, P. Charmont, S. Steuernagel and L. Emsley, *J. Magn. Res.*, 2003, **163**, 105–113.
41 D. H. Zhou, G. Shah, M. Cormos, C. Mullen, D. Sandoz and C. M. Rienstra, *J. Am. Chem. Soc.*, 2007, **129**, 11791–11801.
42 E. Salager, R. S. Stein, S. Steuernagel, A. Lesage, B. Elena and L. Emsley, *Chem. Phys. Lett.*, 2009, **469**, 336–341.
43 K. Takeda, T. Takasaki and K. Takegoshi, *J. Magn. Reson.*, 2015, **258**, 1–5.
44 B. Elena and L. Emsley, *J. Am. Chem. Soc.*, 2005, **127**, 9140–9146.
45 M. Baias, C. M. Widdifield, J.-N. Dumez, H. P. G. Thompson, T. G. Cooper, E. Salager, S. Bassil, R. S. Stein, A. Lesage, G. M. Day and L. Emsley, *Phys. Chem. Chem. Phys.*, 2013, **15**, 8069–8080.
46 S. K. Mazumdar, K. Venkatesan, H.-C. Mez and J. DonohueZhou, *Z. Kristallogr.*, 1969, **130**, 328–339.
47 B. Reif and R. G. Griffin, *J. Magn. Res.*, 2003, **160**, 78–83.
48 D. Zhou and C. Rienstra, *Angew. Chem. Int. Ed.*, 2008, **120**, 7438–7441.
49 K. Mao and M. Pruski, *J. Magn. Res.*, 2009, **201**, 165–174.
50 D. Zhou, J. Shea, A. Nieuwkoop, W. Franks, B. Wylie, C. Mullen, D. Sandoz and C. Rienstra, *Angew. Chem. Int. Ed.*, 2007, **46**, 8380–8383.